Biochemical Engineering Journal 160 (2020) 107638

Contents lists available at ScienceDirect

Biochemical Engineering Journal

journal homepage: www.elsevier.com/locate/bej

Regular article

CHO cell productivity improvement by genome-scale modeling and pathway analysis: Application to feed supplements

Zhuangrong Huang[a], Jianlin Xu[b,**], Andrew Yongky[b], Caitlin S. Morris[a], Ashli L. Polanco[a], Michael Reily[c], Michael C. Borys[b], Zheng Jian Li[b], Seongkyu Yoon[a,*]

[a] Department of Chemical Engineering, University of Massachusetts Lowell, Lowell, MA 01854, USA
[b] Biologics Process Development, Bristol-Myers Squibb, Devens, MA 01434, USA
[c] Research and Development, Bristol-Myers Squibb, Princeton, NJ 08543, USA

HIGHLIGHTS

- A genome-scale CHO model was employed to analyze the metabolism of CHO cells.
- Flux analysis results from genome-scale model were compared with transcriptomics analysis.
- In silico simulations using genome-scale model were performed for feed optimization.
- This is the first study to apply genome-scale CHO model to improve the IgG production.

ARTICLE INFO

Keywords:
GS CHO-K1 cells
Genome-scale model
Cellular metabolism
Feed improvement
Model simulation
Pathway analysis

ABSTRACT

Effective bioprocess development using Chinese hamster ovary (CHO) cells as hosts is hampered by the limited understanding of cellular metabolism under process conditions in bioreactors. Systematic tools such as genome-scale models have been developed, but their value has not been satisfactorily demonstrated and exploited for process development. In this study, we proposed a method using a genome-scale model to analyze existing process studies for bioprocess optimization. First, we used existing industrial CHO cell culture experiments to systematically gain metabolic insights for bioprocess development. Two fed-batch cultures, using the same cell line and process, resulted in different titers by supplementing two different types of feed media. A genome-scale model was applied to calculate fluxomics (i.e., intracellular fluxes) from extracellular metabolomics and then the metabolic differences were further analyzed through pathway analysis between these two cell culture conditions. Transcriptomics data from RNA-Seq were employed at this point for comparison and found to be consistent in pathway analysis with the flux analysis results. At the second stage, we developed a modeling-based approach for media optimization to increase antibody production based on the understanding from the first stage. The new design was tested *in silico* using a genome-scale model and then verified experimentally, confirming the applicability of this modeling-based approach for bioprocess optimization. The framework proposed in this study can maximize the utilization of existing process studies and minimize the time consumed for empirical work in developing new processes.

1. Introduction

Chinese Hamster Ovary (CHO) cells continue to be the most widely used mammalian host for the industrial production of biopharmaceutical products such as monoclonal antibody (mAb) [1–3]. There has been significant improvement in protein production through cell line engineering [4–7] and media optimization [8–11] and remains a major bioprocess development activity in the biopharmaceutical industry. Typically, once a highly productive clone has been generated and evaluated, cell culture process development will move forward to increase productivity and maintain product quality through optimization of media and feed compositions, feeding strategy, and bioprocess conditions [12,13]. Traditional approaches to optimize cell culture include statistical design (e.g., design of experiments (DoE)) [14] and spent

* Corresponding author.
** Corresponding author.
E-mail addresses: jianlin.xu@bms.com (J. Xu), Seongkyu_Yoon@uml.edu (S. Yoon).

https://doi.org/10.1016/j.bej.2020.107638
Received 5 January 2020; Received in revised form 11 April 2020; Accepted 11 May 2020
Available online 16 May 2020
1369-703X/

media analysis [15]. These methods are typically experimentally-based and generally time-consuming [16]. Since antibody synthesis is a biological process that occurs within the cells, cell physiology needs to be characterized to gain a fundamental understanding of the CHO cell metabolism that is associated with high production, and thus such knowledge can be used for optimizing bioprocesses.

High-throughput omics-based technologies have been actively used in recent research to obtain a comprehensive understanding of CHO cell physiology under industrially relevant conditions [8,17–20]. The collection of omics data has found some successes in supporting a number of bioprocess improvement efforts [19]. Each omics data type usually provides a snapshot of a particular layer of complex cellular regulations, such as transcriptome, proteome, and metabolome. It is then important to integrate the information from those multi-omics data to obtain a holistic view of the cell physiology and use the unveiled knowledge to facilitate cell culture optimization strategy for industrial bioprocesses.

Intracellular fluxes represent the metabolic activity within the cell and reflect the complex dynamic interactions between genes, transcripts, proteins, metabolites, enzymatic regulation, and the extracellular environment. Therefore, the analysis of intracellular fluxes can complement other omics studies. Isotope tracing analysis has been widely used to determine intracellular fluxes but it only focuses on specific metabolic networks (e.g., central carbon metabolism) [21–28]) and is not able to provide a systematic perspective of cellular metabolism on a genome-scale network. Whereas, the recently constructed CHO genome-scale metabolic network allows for an in-depth understanding of CHO cell physiology. Three cell line specific genome-scale CHO models (i.e., CHO-K1, CHO-S, and CHO-DG44) have been developed so far and considered all of the currently known conversions of substrates into metabolic products for CHO cells [29]. Genome-scale CHO models have been applied to explore the impact of cellular transfection on global cellular adaptation and protein production [30], and to predict cell phenotypes and known auxotrophies in CHO cells [29].

The idea of applying the genome-scale model for media optimization has been proposed in previous review papers [16,31]. Several studies have provided insights into cellular metabolism of culture phenotype but have not yet used the insights to guide new culture designs [30,32,33]. Motivated by that, we performed this study to demonstrate how the genome-scale model can be applied to process optimization for production improvement and validate the design by experiments. In this work, we introduced a two-stage methodology to gain in-depth process understanding. The first stage incorporates pathway analysis and then the second stage optimizes the bioprocess through model simulation. At each stage, a genome-scale metabolic model was employed. The approach presented in this study shows a novel way to help other researchers understand the cell culture process and effectively accelerate the optimization process for achieving higher productivity by the aid of a genome-scale model.

2. Materials and methods

2.1. Cell line, media and cell culture process

A CHO-K1 GS knockout cell line was used for expression of a proprietary recombinant monoclonal antibody. Proprietary chemically defined seed, basal and feed media were used in this study unless otherwise specified. The feed A (low amino acids (AAs)) was the control feed, while the feed B (high AAs) was the control feed with a higher concentration of 4 amino acids, e.g., serine, lysine, threonine, and tyrosine (Fig. 1). It is important to mention that these four amino acids and the level of increase in the concentration were determined and optimized by performing early screening experiments in an internal high-throughput system. All CHO seed cultures were started from the vial thaw of a frozen vial of master cell bank and passaged in a seed medium containing methionine sulfoximine (MSX). The seed cultures were inoculated to 5 L production bioreactors at 1.5 × 10^6 cells/mL. The fed-batch production cultures were controlled at 36.5 °C. The bioreactor pH was controlled within the range of 6.6–7.6 by the addition of CO_2 gas to decrease pH or addition of 1 M Na_2CO_3 base to increase pH as needed. The DO was maintained at 40% of air saturation by sparging with oxygen. Feeding at 3.5% (v/v) of the initial volume was started on day 2 when appropriate viable cell density (VCD) was achieved and fed daily thereafter. Concentrated glucose stock solution (300 g/L) was supplemented daily as a bolus to bring glucose level back to 5 g/L if its concentration falling below a proprietary level throughout the production run. The added volume of glucose was calculated daily as needed. All experiments were performed in duplicate cultures.

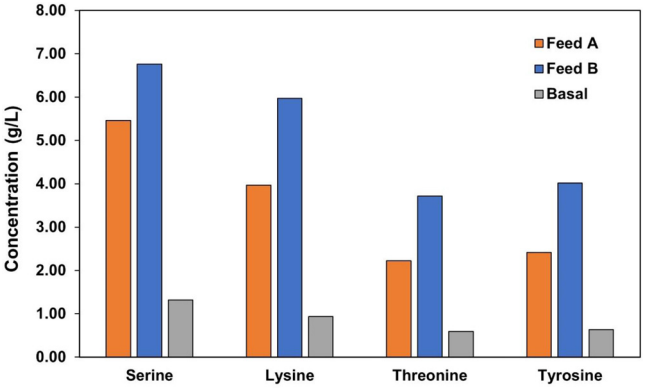

Fig. 1. Serine, lysine, threonine and tyrosine concentrations in production basal medium, feed A (low AAs) and feed B (high AAs). In this study, the amino acid measurements in basal and feed media were performed once, and the results were consistent with the in-house formulation for the medium.

VCD and cell viability were quantified off-line using a Vi-CELL XR automatic cell counter (Beckman Coulter). Glucose, glutamine, glutamate, lactate, and ammonia were quantified with a CEDEX Bio HT analyzer (Roche). A Protein A HPLC was used to measure the protein titer [12]. The protein titer for the condition using feed B with high AAs was set as 100 % to normalize titer within this study. Off-line pH, pCO_2 and pO_2 were monitored daily using a Bioprofile pHOx analyzer (Nova Biomedical). In this study, the fed-batch process was divided into two main metabolic phases based on VCD profiles. The first phase is the exponential growth phase in which the VCD increases exponentially (days 0–6). The second phase is a stationary phase in which the VCD remains approximately constant and the culture viability is always higher than 80% (days 6–10).

2.2. Quantification of extracellular metabolites

Cell culture samples from days 0, 2, 4, 6, 8, 10 were centrifuged at 1000 ×g for 10 min and the cell-free supernatant was stored at -80 °C before analysis. Amino acid concentrations in the supernatant were analyzed by UPLC. The supernatant samples were diluted in Milli-Q water containing an internal standard (sample diluent). The derivatization reagent (Waters AccQ•Tag Ultra Derivitization Kit, Cat#186003836), 6-aminoquinolyl-N-hydroxysuccinimidyl carbamate, was added into the diluted samples for reaction by vortexing at 55 °C for 10 min. The samples were then separated by RP-UPLC (Waters AccQ•Tag Ultra RP Column, Cat# 186003837); the derivatized amino acids were detected at 260 nm as they eluted from the column.

TCA (citrate acid cycle) intermediates including citrate, a-ketoglutarate, succinate, fumarate, malate, and isocitrate were determined in supernatant samples by a method combining NMR and LC/MS at Bristol-Myers Squibb. The detailed sample preparation and analytical procedures are described in the Materials and Methods section in a previous study [34]. The specific oxygen uptake rate (OUR) was also

determined with the method as described in the previous studies [35,36].

2.3. Transcriptome analysis

The cell samples for RNA-Seq analysis were collected at day 6 and day 10, which corresponded to the exponential growth phase and stationary phase, respectively. Approximately 5×10^6 cells were separated from culture broth by centrifugation at 1000 ×g and 4 °C for 10 min. The cell pellets were then washed with 20 mL of ice-cold PBS. The PBS was subsequently removed by centrifuging at 1000 ×g and 4 °C for 10 min. Then the cell pellets were immediately frozen in dry ice and stored at −80 °C. The detailed information of RNA isolation and sequencing can refer to [20]. From the 26,520 genes identified from the global RNA-Seq data, we focused on the metabolic genes associated with the global CHO genome-scale model. As a result, 1728 genes can be mapped to the global CHO genome-scale model developed by researchers in 2016 [29]. For the statistical analysis of the gene expression, ANOVA (Analysis of variance) method was used to calculate the p-value between conditions. A gene was considered to be differentially expressed across conditions if the calculated p-value was less than 0.05.

2.4. Metabolic data processing for flux constraints

The uptake and secretion rates of metabolites (i.e., amino acids, glucose, lactate, ammonium) were calculated from time-series extracellular metabolite concentrations using the following equations (Eqs. (1) and (2)).

$$\mu = \frac{1}{X}\frac{dX}{dt} \tag{1}$$

$$C_i^{t2} - C_i^{t1} - \frac{V_f \times C_i^f}{V} = q_i \int_{t1}^{t2} X dt \tag{2}$$

where X is the VCD; C_i^{t2} and C_i^{t1} are the concentrations of the ith metabolite at time points $t2$ and $t1$, respectively; V_f is the total volume of feed added; V is the working volume of bioreactor; C_i^f is the concentration of the ith metabolite in the feed. The μ, q_i represent the specific cell growth rate, secretion (if calculated q_i is positive) or uptake (if calculated q_i is negative) rate of the ith extracellular metabolite, respectively. The average specific rates were obtained from a plot of the total amount of production/consumption against the total integral viable cell number using linear regression [33].

2.5. Flux balance analysis using genome-scale models

A genome-scale CHO-K1 model was employed to analyze the metabolism of CHO cells in fed-batch culture experiments supplemented with either low AAs or high AAs feeds. This model contains 1298 genes, 4723 reactions, and 2773 metabolites (available from http://bigg.ucsd.edu/). The model accounts for multiple subcellular compartments, including extracellular compartment, cytosol, mitochondria, mitochondrial intermembrane, nucleus, endoplasmic reticulum, lysosome, peroxisome, and the Golgi complex [29]. Flux balance analysis (FBA) was used to calculate the intracellular metabolic fluxes by the optimization of a defined biological objective function using linear programming. The genome-scale model can be represented by a stoichiometric matrix (S) of size m× n (where m is the number of metabolites and n is the number of reactions) and a vector of reaction fluxes (v) [37]. Under the assumption of quasi-steady state, the mass balance equations are given by S× V= 0 [38,39]. To obtain the solution, the model was further constrained by the boundaries of each flux. The upper bound was set to 1000 for all reactions. While the lower bound was set to -1000 or 0 for reversible reactions and irreversible reactions, respectively [29].

The specific metabolic rates from Section 2.4 were used as experimental metabolic constraints. These metabolites include 22 amino acids, glucose, lactate, and ammonium, and are exchanged between intracellular and extracellular environment. The upper and lower bounds of these exchange reactions were set to the measured rates. During the exponential growth phase, the calculated specific IgG productivity was also used as a constraint, and the flux distribution was obtained by maximizing the flux through the biomass reaction. During the stationary phase, where the cell growth was close to zero, flux solutions were obtained by maximizing the reaction rate of IgG biosynthesis [40]. In this study, we utilized the default values from [29] for the boundaries of other fluxes including oxygen consumption [29].

The Constraint-Based Reconstruction and Analysis (COBRA) toolbox was used for FBA analysis in this study [41,42]. Gurobi solver (https://www.gurobi.com/) was applied to solve LP optimization problems. MATLAB (Matlab 2016a; Mathworks, Natick, MA, USA) was used for ANOVA and running COBRA toolbox.

2.6. Pathway analysis

Gene expression levels (of differentially expressed genes identified in Section 2.3) or flux values were considered significantly different when their fold-change in the high AAs cultures compared to the low AAs cultures was at least 1.3. It is important to note that the threshold is user-defined. In previous studies, different fold-changes from 1.2 to 1.5 or higher have been used [43–45]. A web server KOBAS 3.0 was used to evaluate the pathway enrichment analysis [46]. In KOBAS, the input is a set of identified genes that are mapped to known metabolic pathways. The output is a list of significantly enriched pathways using a hypergeometric test. The resulting p-values in enrichment analysis are adjusted for multiple testing using the Benjamini-Hochberg method [47]. The Kyoto Encyclopedia of Genes and Genomes (KEGG) pathway database of Cricetulus griseus (Chinese hamster) was employed during the analysis. In this study, the pathways with p-value < 0.05 were considered as significantly enriched.

3. Results and discussion

The workflow proposed in this study is shown in Fig. 2. A flux balance analysis was conducted to determine how metabolism varied under the two different feed media conditions. The extracellular metabolic consumption or production rates were first calculated from the time-series metabolite concentrations in culture supernatant and the intracellular fluxes were subsequently calculated based on the extracellular metabolic rates and a genome-scale model. By analyzing the flux values, we evaluated the impact of feed media and determined the affected metabolic pathways. The pathway analysis results were also compared with those from RNA-Seq data. In the genome-scale model, transport reactions were used to connect metabolites between extracellular and intracellular compartments. Thus, the impact of changes in extracellular metabolites on cell growth or antibody production can be simulated. Specifically, changes in the extracellular concentration of metabolites (e.g., in cell culture media or feed) can modulate the uptake flux of these metabolites, which in turn impact the relevant transport reactions [48]. The results presented here represent an industrial case study of bioprocess development in CHO cell cultures. Notably, the approach presented in this study including genome-scale modeling and pathway analysis is generic and can be applied to other cell culture conditions.

3.1. Antibody production and extracellular metabolic profiles

In this study, a CHO-K1 cell line was cultured in 5 L fed-batch bioreactors with two different types of feeds. The feed design was described in the Materials and Methods section and the cultures will be respectively called low AAs cultures (with feed A) and high AAs cultures (with feed B). Feed medium was added daily throughout the culture starting on day 2. Fig. 3 shows the profiles of VCD, cell viability,

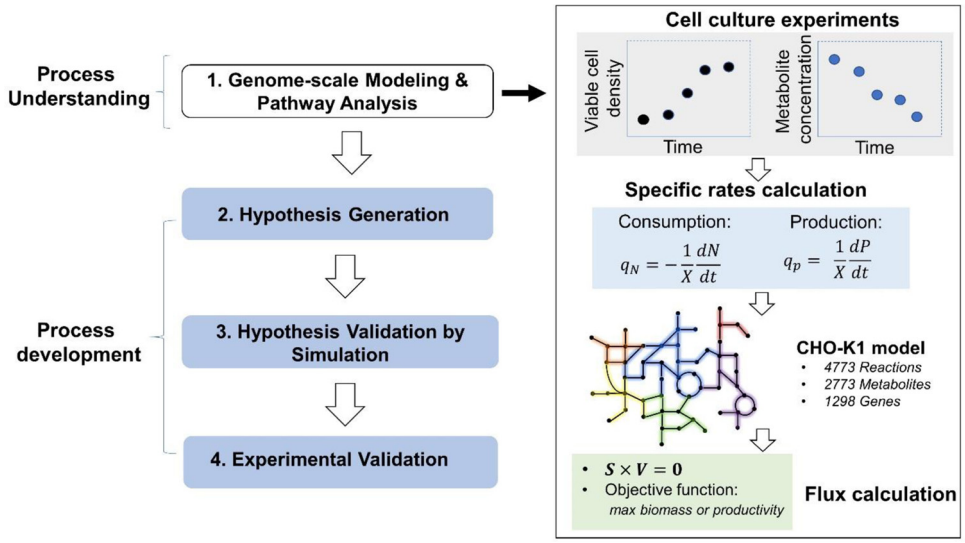

Fig. 2. Workflow for the combined systems biology and genome-scale modeling approach. X, P, and N stand for the VCD, product, and nutrient concentration, respectively.

IgG production, glucose, glutamine, lactate, and osmolality for all fed-batch cultures (in view of the fed-batch process in this study, the total amount based profiles were also provided and can be seen in Fig. S1). As shown in Fig. 3A, the VCD reached its peak around day 6, and after that the cultures transitioned from exponential growth to the stationary phase. Interestingly, the low AAs and high AAs cultures had very similar VCD profiles at both the exponential phases (before day 6) and the stationary phases (from day 6 to day 10). This indicates that the different feeds, low AAs and high AAs, did not significantly affect cell growth (before day 10). The two cultures showed similar IgG production titer during the exponential phase, but during the stationary phase, production was higher in the high AAs cultures (Fig. 3C). In contrast, the two cultures diverged significantly after day 10. The low AAs cultures exhibited a rapid decline in VCD (Fig. 3A) and viability (Fig. 3B), lactate continued to accumulate to high levels and IgG titer (Fig. 3C) leveled off compared to the high AAs cultures.

CHO cells take up glucose as a major carbon source and release byproducts such as lactate through glycolytic metabolism [21,49]. According to the profiles of VCD (Fig. 3A) and glucose (Fig. 3D), it was found that low AAs and high AAs cultures had similar glucose uptake patterns during the exponential growth phase, but it substantially differed during the stationary phase. These results were also verified by a statistical analysis of the glucose specific uptake rates, respectively, at the exponential and stationary phases from the two feed conditions (as seen in Fig. S2). Glutamine is a major energy source, nitrogen donator for many anabolic pathways [50]. In this work, glutamine was not supplemented in the culture medium and was intracellularly synthesized using the enzyme glutamine synthetase to meet the cell growth and productivity requirements. According to Fig. 3E, there was minimal difference in the glutamine profile between the two conditions before day 10. During the exponential phase, lactate accumulation was similar for the two cultures. However, near the end of the exponential phase, the lactate profiles were distinct as lactate shifted from production to consumption in the high AAs cultures, while this shift did not occur in the low AAs cultures (Fig. 3F). There has not been an explicit understanding of the mechanisms behind the lactate switch, however, a number of studies have pointed to a productivity increase in cultures that undergo metabolic shift with lactate [51]. Indeed, our study also indicated the positive relationship between lactate shift with IgG productivity.

It is important to focus the study on cellular metabolism during the stationary phase (day 6–10) where different productivities were first

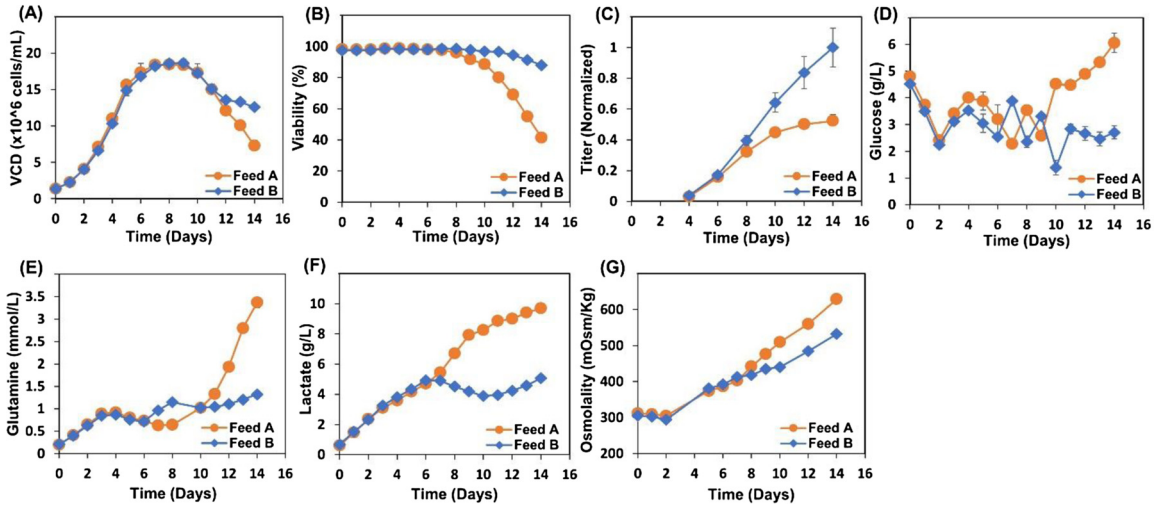

Fig. 3. Cell culture experimental data used for the genome-scale model at 5 L bioreactor scale ($n = 2$). (A) Time-series viable cell density. (B) Cell viability. (C) Time-series mAb production. (D) Time-series glucose concentration. (E) Time-series glutamine concentration. (F) Time-series lactate concentration. (G) Osmolality.

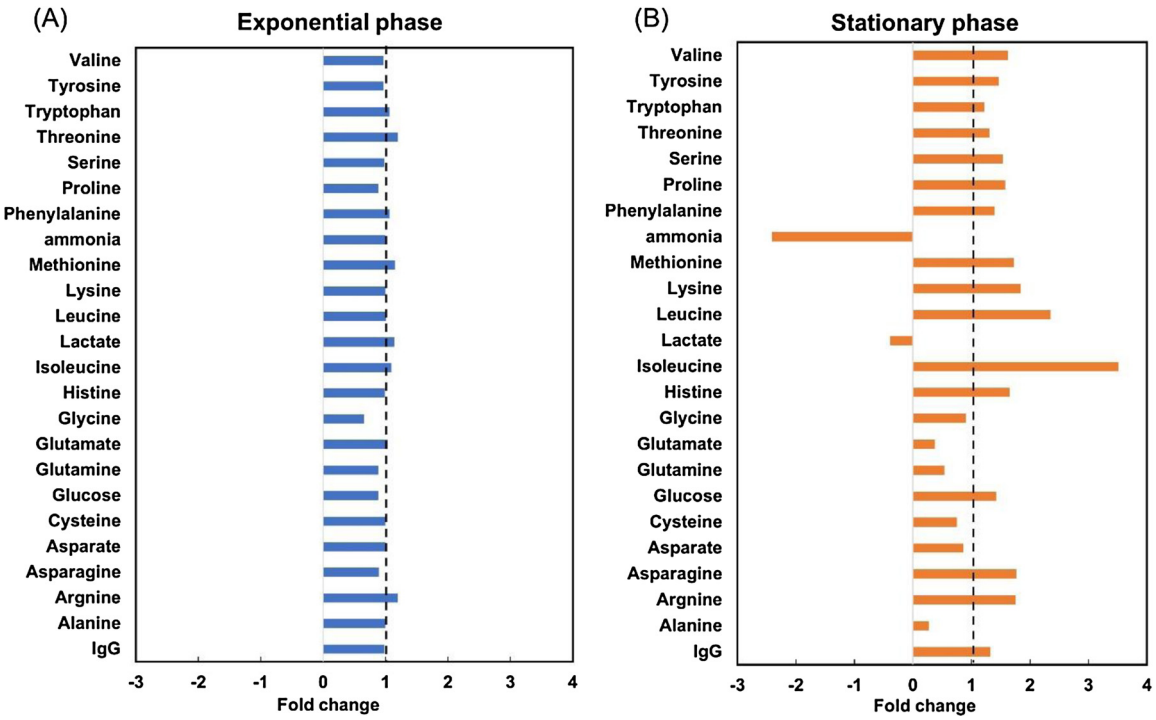

Fig. 4. Comparison of experimentally measured specific rates between cultures of low AAs and high AAs at different culture phases: (A) Exponential phase, (B) Stationary phase. The x-axis represents fold change of specific rates which was calculated by the value in high AAs cultures divided by the value in low AAs cultures.

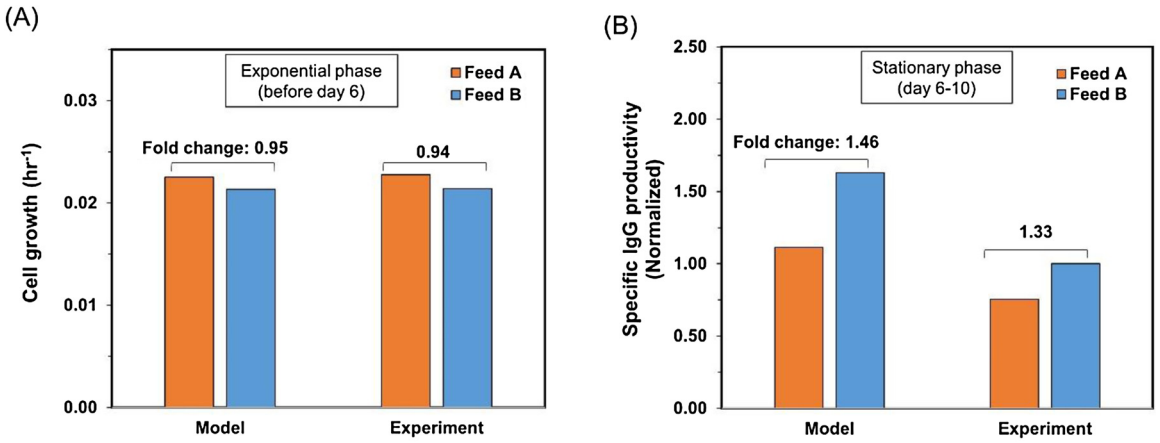

Fig. 5. Comparison of experimental measured and predicted values by genome-scale model for cell growth during exponential phase (A) and specific IgG productivity during stationary phase (B), respectively. The values on top of the bars represent the fold change of cell growth and productivity between low AAs (Feed A) and high AAs (Feed B) cultures. The fold change was calculated by the value in high AAs cultures divided by the value in low AAs cultures.

observed and understand how the feeds affect the metabolic pathways. Such an understanding will enable the design of new feeds to engineer culture processes. The impact from stationary phase would prolong after day 10, however, additional negative impacts on cell viability and productivity were imposed on low AAs cultures including the high accumulation of lactate and rise of osmolarity as widely known in literature (as seen in Fig. 3F and G) [51,52].

3.2. Specific consumption and production rates of metabolites

The specific rates of amino acid consumption and production are shown in Fig. 4. One could expect that enriched nutrient feed would result in higher specific uptake rates. However, during the exponential phase, the uptake rates for serine, threonine, tyrosine, and lysine remained similar in the two cultures regardless of the concentration of these amino acids in the feeds (Fig. 4A). Whereas, during the stationary phase the uptake and production rates showed major rearrangements in amino acid metabolism from the two different feed conditions (Fig. 4B). Interestingly, not only the four amino acids but also the rates for nearly all amino acids were increased. This global adaptation of amino acid metabolism triggered by the four amino acids indicates the inter--regulation among amino acids [53]. These effects are facilitated via a series of mechanisms. For example, individual amino acid transporters can facilitate the import of multiple amino acids, while for a given amino acid, multiple transporters might be involved in its transport [48]. A recent study also found that the transport rates of selected amino acids are highly correlated with the relative concentration of competing amino acids in CHO cell culture [48].

3.3. Flux calculation based on genome-scale CHO models

Next, we calculated steady-state metabolic fluxes using the genome-

scale model that was previously developed for a CHO-K1 cell line [29]. The metabolic model was constrained using experimentally determined specific uptake and production rates. In the model, the maximization of biomass (during exponential phase) and IgG productivity (during stationary phase) were used as objective functions to obtain the optimal flux solution [29]. Fig. 5 shows the cell growth and productivity predicted by the model and measured by experiments for the exponential phase (Fig. 5A) and stationary phase (Fig. 5B), respectively. As shown in Fig. 5A, the two cultures had very similar predicted cell growth rates during the exponential phase; this result was consistent with the experimental measurements. In addition, we saw an increase of predicted IgG productivity (46%) under enriched high AAs compared to low AAs (left bars, Fig. 5B). This magnitude was comparable with the experimental results that showed an increase of 33% (right bars, Fig. 5B). This consistency between model simulation and experimental observation has notable importance for the following in silico simulation for feed design because genome-scale modeling has been demonstrated to be able to predict phenotypes [29].

3.4. Pathway analysis from genome-scale model and RNA-Seq data

Pathway analysis was carried out to determine how the enriched four amino acids added in the feed affected the metabolism to promote IgG production. Only the reactions with non-zero flux values in at least one sample were considered. Since there was no distinction for the flux distribution during the exponential phase between the two cultures (which was consistent with the metabolic profiles as shown in Fig. 3 before day 6), the detailed analysis of fluxes was only focused on the stationary phase in this study. Significant changes in many reactions were observed under the stationary phase, for example, glycolysis/gluconeogenesis, oxidative phosphorylation, and the TCA cycle. Given the complexity of comprehensive analysis in each reaction, we performed pathway enrichment analysis. In the analysis, the differed fluxes were identified in the high-producing (high AAs) cultures against the low-producing (low AAs) cultures with a 1.3-fold change cutoff. This analysis identified several significantly enriched pathways with a p-value < 0.05. As seen in Fig. 6A, the most active pathways were N-glycan biosynthesis, glycolysis/gluconeogenesis, valine, leucine and isoleucine degradation, TCA cycle, alanine metabolism, and amino sugar and nucleotide sugar metabolism. Our results thus suggest that N-glycan biosynthesis was highly active in the enriched amino acid feed condition which is consistent with our experimental observation that IgG productivity increased in high AAs cultures. Additionally, the pathways of valine, leucine and isoleucine degradation and TCA cycle were found to be enriched significantly in the high-producing cultures, as shown in Fig. 6A. This links to the understanding that branched chain amino acids (BCAAs, i.e., leucine, valine, isoleucine) can serve as alternative energy sources by producing energy-rich intermediates for the TCA cycle [54–57]. A metabolic connection between four amino acids, BCAAs and TCA cycle can be seen in Fig. 7.

To confirm the pathway analysis results from flux values, the same approach of pathway enrichment analysis was applied to the gene expression data obtained by RNA-Seq. Transcriptomic analysis was carried out with samples collected at day 6 and day 10. The multi-dimensional scaling (MDS) plots in Fig. S3 indicated similar gene expression was observed at the end of the exponential growth phase (day 6). Accordingly, there are only a few genes identified as differentially changed genes (with the method in Section 2.6) and negligible pathways enriched between low AAs and high AAs cultures (data not shown). These results are consistent with the metabolic profiles of day 6 as seen in Fig. 3. At day 10, the gene expression varied significantly between high AAs and low AAs cultures, as shown in the MDS plot (Fig. S3), where the transcriptomes of these two cultures could be distinguished along with the first principal component. Several pathways were enriched in high AAs cultures (Fig. 6B) and most of them were overlapping with the pathways found in Fig. 6A (these pathways are marked by asterisk). Among these pathways, the pathway of BCAAs (valine, leucine, and isoleucine) degradation was most closely correlated with the four amino acids (Fig. 7A). In summary, the pathway analysis in Fig. 6 indicates that TCA metabolism was enriched in high AAs cultures compared to low AAs cultures as a result of the high amount of four amino acids supplemented in the feed.

We further analyzed the TCA activity by measuring the concentration of citrate, a-ketoglutarate, succinate, fumarate, malate, and isocitrate, which are the TCA intermediates present in the extracellular environment. As shown in Fig. 8, the relative concentration of these TCA intermediates is similar between the two cultures up to day 6. As the cultures continued and passed day 6, high AAs cultures demonstrated a substantial increase in citrate, a-ketoglutarate, succinate, fumarate, and malate. The fact that the concentration of these metabolites was increased to different extents in high AAs cultures is likely due to the higher supplementation of four amino acids, which supports the results of pathway analysis. Only the metabolite of isocitrate had similar concentration profiles between the two cultures. One explanation is that citrate (which is the precursor of isocitrate) was substantially consumed in high AAs cultures. Our pathway analysis coincidently shows that fatty acid metabolism was enriched in high AAs cultures, indicating that a high amount of citrate might have been used for fatty acid synthesis. In addition, OUR was observed to be significantly elevated in the high AAs cultures (Fig. 9), which further confirms a high activity of energy metabolism in the high AAs cultures.

3.5. Identification of bioprocess targets for productivity improvement

In this section, we used the genome-scale model to perform process optimization by simulating amino acid supplementation. To start with, a proof-of concept study was made using the genome-scale model to simulate a scenario of the improvement achieved in the high AAs cultures from the low AAs cultures by modulating the uptake rates of the four amino acids (i.e., serine, threonine, tyrosine, and lysine). Specifically, we constrained the genome-scale model with measured extracellular consumption/uptake rates from low AAs cultures, then assigned a higher uptake value for these four amino acids while keeping the values for other constraints unchanged. In this study, the uptake rates were increased by 50% and this percentage value was generated by comparing the measured rates between high AAs and low AAs cultures. As shown in Fig. 10, the simulated specific IgG productivity from the optimized culture (the middle bar) increased from that in the low AAs cultures (shown as the left-most bar in Fig. 10). It was previously shown that the high AAs cultures with high amount of four amino acids in the feed achieve a higher mAb production compared to the low AAs cultures (Fig. 3B). Therefore, our *in-silico* result was consistent with the experimental observations.

Based on the first success in the above tests, we now aimed to identify new targets (which were not tested in the previous simulation) to further improve the IgG production. According to the pathway analysis in Section 3.4, the pathway of valine, leucine and isoleucine degradation was enriched in the high AAs cultures due to the high concentration of the four amino acids in the feed (Fig. 7A). It has been reported that the degradation of valine, leucine, and isoleucine contributes to intermediates of the TCA cycle to produce energy [58,59]. Coincidentally, the pathway analysis also revealed that the TCA cycle was enriched in high AAs cultures as shown in Fig. 6. Therefore, we asked whether increased valine, leucine and isoleucine uptake rates could also contribute to the degradation for energy production as the new feed design seen in Fig. 7B.

Then, we tested the above hypothesis *in silico* using model simulation. We predicted IgG productivity during the stationary phase by increasing the uptake rate by 50% for leucine, isoleucine, and valine in the new simulation. Because isoleucine intake was already large in high AAs cultures (Fig. 4B) and can be additionally converted from threonine that was added daily from day 2 (Fig. 1), isoleucine is no longer

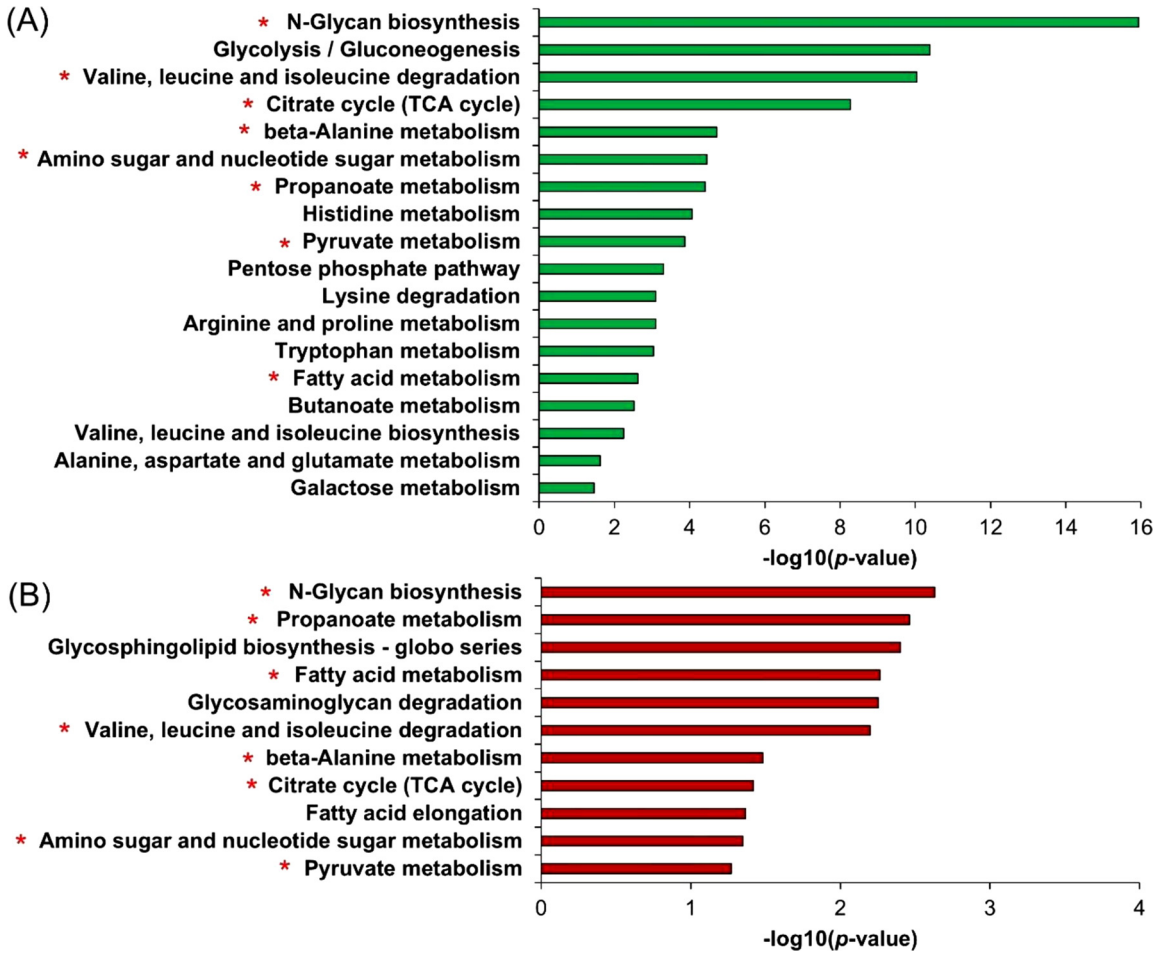

Fig. 6. Pathway analysis with the data from flux balance analysis (A) and measured RNA-Seq data (B) according to the minus log transformation of the *p*-value. All the reactions shown in the figure have achieved a significance value of non-log scale *p*-value < 0.05 (equivalent to a score greater than 1.3 on *x*-axis). The asterisk indicates the pathway is enriched both in figure A and B.

considered in our new design to be supplemented to avoid over-dosage. Only leucine and valine are designed to be added in simulation. The simulation showed that leucine and valine addition in the feed (third bar in Fig. 10) can further improve the productivity by appropriately 19% apart from the known four amino acids (middle bar in Fig. 10). We also found that the simulation results were similar under the conditions of increasing leucine, isoleucine and valine (data not shown). Taken together, leucine and valine were identified as the new targets in feed

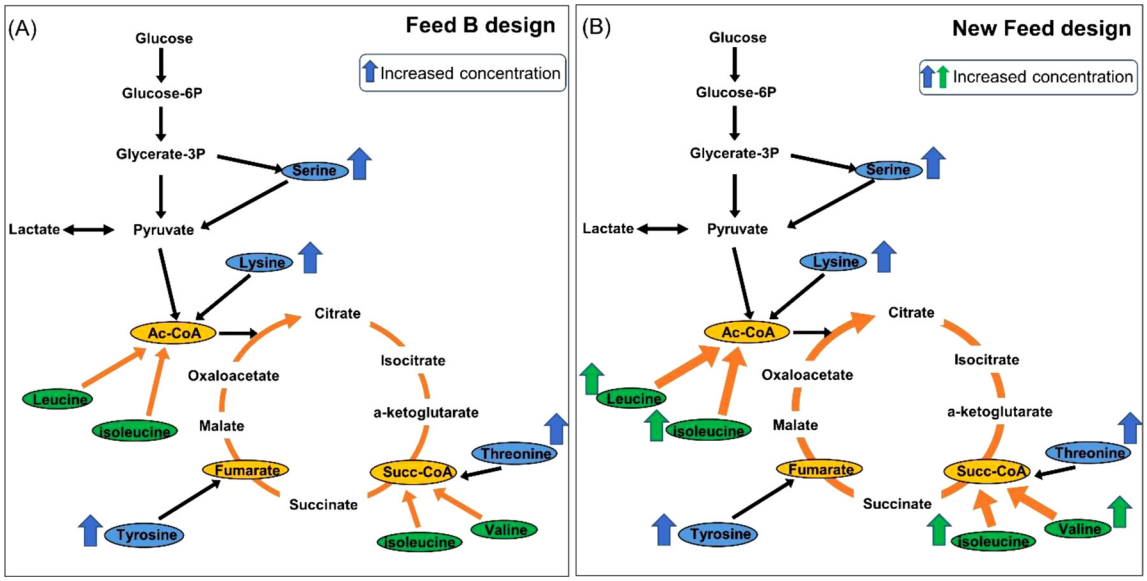

Fig. 7. Schematics of high AAs (Feed B) cultures design and new feed design.

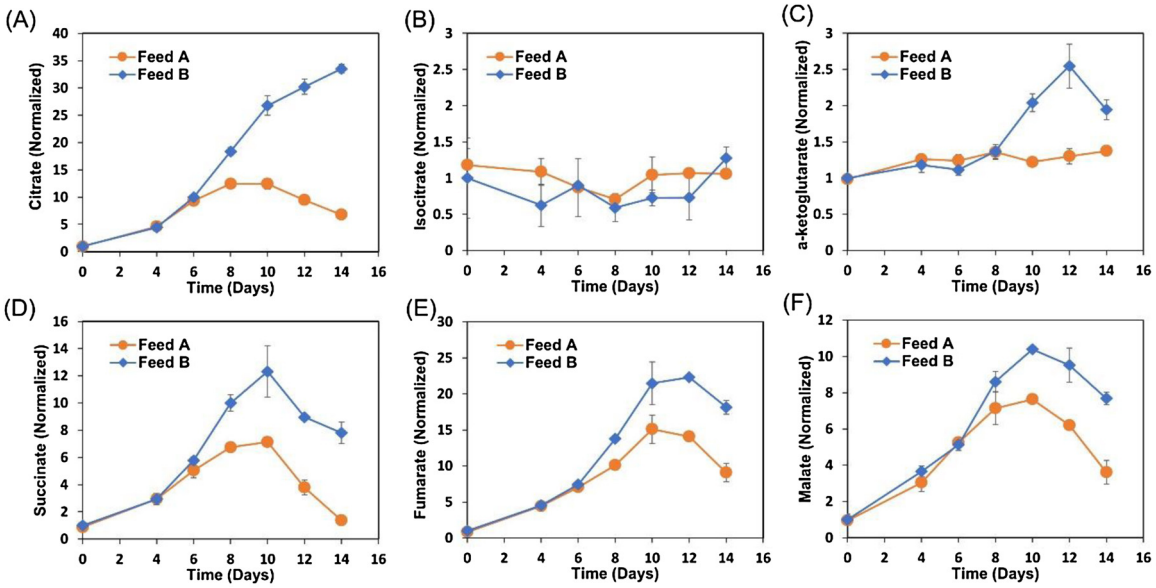

Fig. 8. The concentration of TCA intermediates in the supernatant of low AAs (Feed A) and high AAs (Feed B) cultures at 5 L bioreactor scale (n = 2). (A) Citrate. (B) Isocitrate. (C) a-ketoglutarate. (D) Succinate. (E) Fumarate. (F) Malate. The concentration of each metabolite at day 0 in high AAs cultures was set as 100% to normalize data from different time points.

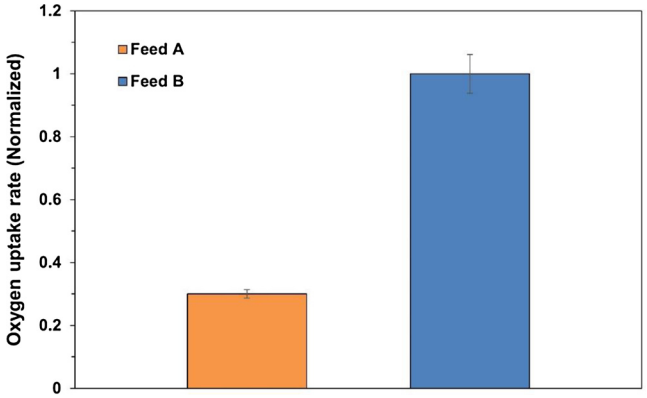

Fig. 9. The comparison of oxygen uptake rates (OUR) between high AAs (Feed A) and low AAs (Feed B) cultures during the stationary phase.

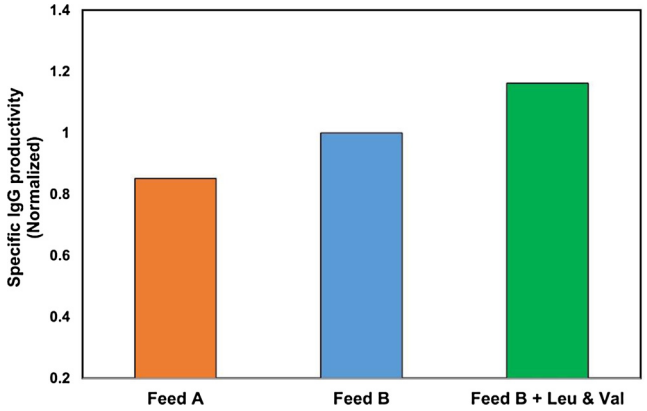

Fig. 10. Simulation results for feed design using genome-scale modeling for control feed (Feed A), increased concentration of four amino acids (Ser, Lys, Thr, Tyr) (Feed B), and increased concentration of six amino acids (Ser, Lys, Thr, Tyr, Leu, Val) (Feed B + Leu &Val).

design to further increase productivity.

3.6. Experimental validation with new feed design

The final step of the workflow was to operate bioreactors runs with the same process setting used as the previous low and high AAs cultures. A new feed design (higher amount of leucine and valine added to feed B) as shown in Table 1 was implemented. The cell culture with high AAs (Feed B) was used as the control. All experiments were performed in duplicate cultures. A statistically significant difference in titer was observed between control and validation cultures (p-value ≤ 0.05, one-way ANOVA). The validation experiments showed that new amino acids supplementation in the feed resulted in an average titer increase of 11.8% compared to the high AAs cultures, in agreement with the stated hypothesis of the feed design from *in silico* simulation (Table 1). The other cell culture performance, including VCD, viability, lactate, and other metabolic profiles were found similar between the control and validation experiments (data not shown).

It has been known that genome-scale models have limitations that these models cannot predict metabolite concentration and do not account for regulatory effects [60]. The main hurdle here is how to precisely decide the concentration of amino acids in the feed that can increase the uptake rate for these specific amino acids by a targeted percent. To demonstrate that, it was shown in the data from the high AAs cultures that the higher concentration for the four amino acids did not only affect the uptake of these four amino acids but also regulated the metabolism of other amino acids (Fig. 4B). Future exploration to computationally decipher the quantitative relationship between each amino acid in the metabolism may help tackle this challenge. Furthermore, it has recently been shown that the catabolism of some amino acids can lead to the formation of toxic intermediates [49,61,62].

Table 1
Cell culture design for validation experiments at 5 L bioreactor scale.

Conditions	Feed medium	Normalized titer
Control (n = 2)	Feed B (serine, threonine, tyrosine, lysine)	1
Validation (n = 2)	Feed B (serine, threonine, tyrosine, lysine) +increased Leu & Val	1.12

Beyond that, it is important to consider the interactions between amino acids and other components in media, particularly metal ions [63]. Thus, once identifying the optimization targets from *in silico* simulation, as a natural next step, the amino acid combinations can be optimized by using DoE methods to determine the most effective concentration to enhance the mAb production in future experimental work.

As genome-scale CHO modeling has been applied to analyze nutrient catabolism [32], we demonstrated herethat the genome-scale model can also be used as a qualitative tool to identify targets for media optimization. Although this study represents an important step for genome-scale model application for CHO cells, researchers should keep in mind that a discrepancy between the value predicted in silico and the experiment should be expected. In the future, more detailed and quantitative biochemical information of cellular metabolism may become available. For example, the biomass composition for different CHO cell lines may be measured and applied to formulate more accurate biomass objective functions [64]. With improvements in genome-scale models from various aspects, we will expect an application of genome-scale models more quantitatively and effectively for process optimization.

4. Conclusion

Cell culture media and feed optimization is a standard activity during upstream process development. However, how the optimized media affects the metabolism and which pathways contribute to improve mAb production remains difficult to be understood. Here we demonstrated an application of a genome-scale model to answer this question as shown using two different cell culture conditions. New feed design resulted in an improvement in productivity. Our results demonstrate that genome-scale modeling is a promising approach for aiding process understanding and identification of new bioprocess targets for cell culture optimization.

We believe the study presented here is important for bioprocess development. First, it advances the fundamental understanding of amino acid metabolism by demonstrating a link between amino acid changes and IgG production. The important metabolic insights were illustrated by the genome-scale model and validated by transcriptomics analysis. Second, our comprehensive genome-scale model approach can serve as a reference computational tool both for basic process understanding and for *in silico* simulation for cell culture conditions. More importantly, our study included both metabolism analysis and *in silico* model simulation and exemplifies how a systems-level approach can add value to industry for effective bioprocess development.

CRediT authorship contribution statement

Zhuangrong Huang: Methodology, Data curation, Formal analysis, Writing - original draft, Writing - review & editing. **Jianlin Xu:** Supervision, Funding acquisition, Conceptualization, Methodology, Data curation, Writing - review & editing. **Andrew Yongky:** Methodology, Data curation, Writing - review & editing. **Caitlin S. Morris:** Data curation, Writing - review & editing. **Ashli L. Polanco:** Data curation, Writing - review & editing. **Michael Reily:** Data curation, Writing - review & editing. **Michael C. Borys:** Project administration, Writing - review & editing. **Zheng Jian Li:** Project administration, Writing - review & editing. **Seongkyu Yoon:** Supervision, Funding acquisition, Conceptualization, Methodology, Data curation, Writing - review & editing.

Declaration of Competing Interest

The authors declare that they have no known competing financial interests or personal relationships that could have appeared to influence the work reported in this paper.

Acknowledgements

The authors are grateful for the financial support of this work provided by Bristol-Myers Squibb and thank Jia Zhao, Kevin McFarland and Seoyoung Park for supporting some of the lab work.

Appendix A. Supplementary data

Supplementary material related to this article can be found, in the online version, at doi:https://doi.org/10.1016/j.bej.2020.107638.

References

[1] T. Amann, A.H. Hansen, S. Kol, H.G. Hansen, J. Arnsdorf, S. Nallapareddy, B. Voldborg, G.M. Lee, M.R. Andersen, H.F. Kildegaard, Glyco-engineered CHO cell lines producing alpha-1-antitrypsin and C1 esterase inhibitor with fully humanized N-glycosylation profiles, Metab. Eng. 52 (2019) 143–152.
[2] C.C. Kuo, A.W. Chiang, I. Shamie, M. Samoudi, J.M. Gutierrez, N.E. Lewis, The emerging role of systems biology for engineering protein production in CHO cells, Curr. Opin. Biotechnol. 51 (2018) 64–69.
[3] H. Laux, S. Romand, S. Nuciforo, C.J. Farady, J. Tapparel, S. Buechmann-Moeller, B. Sommer, E.J. Oakeley, U. Bodendorf, Degradation of recombinant proteins by Chinese hamster ovary host cell proteases is prevented by matriptase-1 knockout, Biotechnol. Bioeng. 115 (2018) 2530–2540.
[4] A. Druz, Y.J. Son, M. Betenbaugh, J. Shiloach, Stable inhibition of mmu-miR-466h-5p improves apoptosis resistance and protein production in CHO cells, Metab. Eng. 16 (2013) 87–94.
[5] L.A. Pieper, M. Strotbek, T. Wenger, M. Gamer, M.A. Olayioye, A. Hausser, Secretory pathway optimization of CHO producer cells by co-engineering of the mitosRNA-1978 target genes CerS2 and Tbc1D20, Metab. Eng. 40 (2017) 69–79.
[6] M. Strotbek, L. Florin, J. Koenitzer, A. Tolstrup, H. Kaufmann, A. Hausser, M.A. Olayioye, Stable microRNA expression enhances therapeutic antibody productivity of Chinese hamster ovary cells, Metab. Eng. 20 (2013) 157–166.
[7] K. Xiong, K.F. Marquart, K.J. la Cour Karottki, S. Li, I. Shamie, J.S. Lee, S. Gerling, N.C. Yeo, A. Chavez, G.M. Lee, N.E. Lewis, H.F. Kildegaard, Reduced apoptosis in Chinese hamster ovary cells via optimized CRISPR interference, Biotechnol. Bioeng. 116 (2019) 1813–1819.
[8] E. Baek, J.S. Lee, G.M. Lee, Untangling the mechanism of 3-methyladenine in enhancing the specific productivity: transcriptome analysis of recombinant Chinese hamster ovary cells treated with 3-methyladenine, Biotechnol. Bioeng. 115 (2018) 2243–2254.
[9] M. Buchsteiner, L.E. Quek, P. Gray, L.K. Nielsen, Improving culture performance and antibody production in CHO cell culture processes by reducing the Warburg effect, Biotechnol. Bioeng. 115 (2018) 2315–2327.
[10] T.K. Ha, A.H. Hansen, S. Kol, H.F. Kildegaard, G.M. Lee, Baicalein reduces oxidative stress in CHO cell cultures and improves recombinant antibody productivity, Biotechnol. J. 13 (2018) e1700425.
[11] J.H. Park, S.M. Noh, J.R. Woo, J.W. Kim, G.M. Lee, Valeric acid induces cell cycle arrest at G1 phase in CHO cell cultures and improves recombinant antibody productivity, Biotechnol. J. 11 (2016) 487–496.
[12] J. Xu, M.S. Rehmann, X. Xu, C. Huang, J. Tian, N.X. Qian, Z.J. Li, Improving titer while maintaining quality of final formulated drug substance via optimization of CHO cell culture conditions in low-iron chemically defined media, MAbs. 10 (2018) 488–499.
[13] J. Xu, P. Tang, A. Yongky, B. Drew, M.C. Borys, S. Liu, Z.J. Li, Systematic development of temperature shift strategies for Chinese hamster ovary cells based on short duration cultures and kinetic modeling, MAbs 11 (2019) 191–204.
[14] F. Torkashvand, B. Vaziri, S. Maleknia, A. Heydari, M. Vossoughi, F. Davami, F. Mahboudi, Designed amino acid feed in improvement of production and quality targets of a therapeutic monoclonal antibody, PLoS One 10 (2015) e0140597.
[15] E.K. Read, S.A. Bradley, T.A. Smitka, C.D. Agarabi, S.C. Lute, K.A. Brorson, Fermentanomics informed amino acid supplementation of an antibody producing mammalian cell culture, Biotechnol. Prog. 29 (2013) 745–753.
[16] S. Sha, Z. Huang, Z. Wang, S. Yoon, Mechanistic modeling and applications for CHO cell culture development and production, Curr. Opin. Chem. Eng. 22 (2018) 54–61.
[17] Y. Gao, S. Ray, S. Dai, A.R. Ivanov, N.R. Abu-Absi, A.M. Lewis, Z. Huang, Z. Xing, M.C. Borys, Z.J. Li, B.L. Karger, Combined metabolomics and proteomics reveals hypoxia as a cause of lower productivity on scale-up to a 5000-liter CHO bioprocess, Biotechnol. J. 11 (2016) 1190–1200.
[18] C.L. Kim, G.M. Lee, Improving recombinant bone morphogenetic protein-4 (BMP-4) production by autoregulatory feedback loop removal using BMP receptor-knockout CHO cell lines, Metab. Eng. 52 (2019) 57–67.
[19] A.M. Lewis, N.R. Abu-Absi, M.C. Borys, Z.J. Li, The use of' Omics technology to rationally improve industrial mammalian cell line performance, Biotechnol. Bioeng. 113 (2016) 26–38.
[20] S. Sha, H. Bhatia, S. Yoon, An RNA-seq based transcriptomic investigation into the productivity and growth variants with Chinese hamster ovary cells, J. Biotechnol. 271 (2018) 37–46.
[21] W.S. Ahn, M.R. Antoniewicz, Metabolic flux analysis of CHO cells at growth and non-growth phases using isotopic tracers and mass spectrometry, Metab. Eng. 13 (2011) 598–609.
[22] W.S. Ahn, M.R. Antoniewicz, Parallel labeling experiments with [1,2-(13)C]glucose

and [U-(13)C]glutamine provide new insights into CHO cell metabolism, Metab. Eng. 15 (2013) 34–47.
[23] W.S. Ahn, S.B. Crown, M.R. Antoniewicz, Evidence for transketolase-like TKTL1 flux in CHO cells based on parallel labeling experiments and (13)C-metabolic flux analysis, Metab. Eng. 37 (2016) 72–78.
[24] L. Junghans, A. Teleki, A.W. Wijaya, M. Becker, M. Schweikert, R. Takors, From nutritional wealth to autophagy: in vivo metabolic dynamics in the cytosol, mitochondrion and shuttles of IgG producing CHO cells, Metab. Eng. 54 (2019) 145–159.
[25] C.P. Long, J. Au, J.E. Gonzalez, M.R. Antoniewicz, 13C metabolic flux analysis of microbial and mammalian systems is enhanced with GC-MS measurements of glycogen and RNA labeling, Metab. Eng. 38 (2016) 65–72.
[26] A.G. McAtee Pereira, J.L. Walther, M. Hollenbach, J.D. Young, (13) C flux analysis reveals that rebalancing medium amino acid composition can reduce Ammonia production while preserving central carbon metabolism of CHO cell cultures, Biotechnol. J. 13 (2018) e1700518.
[27] N. Templeton, K.D. Smith, A.G. McAtee-Pereira, H. Dorai, M.J. Betenbaugh, S.E. Lang, J.D. Young, Application of (13)C flux analysis to identify high-productivity CHO metabolic phenotypes, Metab. Eng. 43 (2017) 218–225.
[28] N. Templeton, S. Xu, D.J. Roush, H. Chen, (13)C metabolic flux analysis identifies limitations to increasing specific productivity in fed-batch and perfusion, Metab. Eng. 44 (2017) 126–133.
[29] H. Hefzi, K.S. Ang, M. Hanscho, A. Bordbar, D. Ruckerbauer, M. Lakshmanan, C.A. Orellana, D. Baycin-Hizal, Y. Huang, D. Ley, V.S. Martinez, S. Kyriakopoulos, N.E. Jimenez, D.C. Zielinski, L.E. Quek, T. Wulff, J. Arnsdorf, S. Li, J.S. Lee, G. Paglia, N. Loira, P.N. Spahn, L.E. Pedersen, J.M. Gutierrez, Z.A. King, A.M. Lund, H. Nagarajan, A. Thomas, A.M. Abdel-Haleem, J. Zanghellini, H.F. Kildegaard, B.G. Voldborg, Z.P. Gerdtzen, M.J. Betenbaugh, B.O. Palsson, M.R. Andersen, L.K. Nielsen, N. Borth, D.Y. Lee, N.E. Lewis, A consensus genome-scale reconstruction of chinese Hamster ovary cell metabolism, Cell Syst. 3 (2016) 434–443 e8.
[30] F.N.K. Yusufi, M. Lakshmanan, Y.S. Ho, B.L.W. Loo, P. Ariyaratne, Y. Yang, S.K. Ng, T.R.M. Tan, H.C. Yeo, H.L. Lim, S.W. Ng, A.P. Hiu, C.P. Chow, C. Wan, S. Chen, G. Teo, G. Song, J.X. Chin, X. Ruan, K.W.K. Sung, W.S. Hu, M.G.S. Yap, M. Bardor, N. Nagarajan, D.Y. Lee, Mammalian systems biotechnology reveals global cellular adaptations in a recombinant CHO cell line, Cell Syst. 4 (2017) 530–542 e6.
[31] J.M. Gutierrez, N.E. Lewis, Optimizing eukaryotic cell hosts for protein production through systems biotechnology and genome-scale modeling, Biotechnol. J. 10 (2015) 939–949.
[32] C. Calmels, A. McCann, L. Malphettes, M.R. Andersen, Application of a curated genome-scale metabolic model of CHO DG44 to an industrial fed-batch process, Metab. Eng. 51 (2018) 9–19.
[33] X. Pan, C. Dalm, R.H. Wijffels, D.E. Martens, Metabolic characterization of a CHO cell size increase phase in fed-batch cultures, Appl. Microbiol. Biotechnol. 101 (2017) 8101–8113.
[34] A.M. Lewis, W.D. Croughan, N. Aranibar, A.G. Lee, B. Warrack, N.R. Abu-Absi, R. Patel, B. Drew, M.C. Borys, M.D. Reily, Z.J. Li, Understanding and controlling sialylation in a CHO fc-fusion process, PLoS One 11 (2016) e0157111.
[35] Z. Xing, B.M. Kenty, Z.J. Li, S.S. Lee, Scale-up analysis for a CHO cell culture process in large-scale bioreactors, Biotechnol. Bioeng. 103 (2009) 733–746.
[36] Z. Xing, A.M. Lewis, M.C. Borys, Z.J. Li, A carbon dioxide stripping model for mammalian cell culture in manufacturing scale bioreactors, Biotechnol. Bioeng. 114 (2017) 1184–1194.
[37] Z. Huang, D.Y. Lee, S. Yoon, Quantitative intracellular flux modeling and applications in biotherapeutic development and production using CHO cell cultures, Biotechnol. Bioeng. 114 (2017) 2717–2728.
[38] J.D. Orth, I. Thiele, B.O. Palsson, What is flux balance analysis? Nat. Biotechnol. 28 (2010) 245–248.
[39] L.E. Quek, S. Dietmair, J.O. Kromer, L.K. Nielsen, Metabolic flux analysis in mammalian cell culture, Metab. Eng. 12 (2010) 161–171.
[40] S.N. Sou, C. Sellick, K. Lee, A. Mason, S. Kyriakopoulos, K.M. Polizzi, C. Kontoravdi, How does mild hypothermia affect monoclonal antibody glycosylation? Biotechnol. Bioeng. 112 (2015) 1165–1176.
[41] S.A. Becker, A.M. Feist, M.L. Mo, G. Hannum, B.O. Palsson, M.J. Herrgard, Quantitative prediction of cellular metabolism with constraint-based models: the COBRA Toolbox, Nat. Protoc. 2 (2007) 727–738.
[42] J. Schellenberger, R. Que, R.M. Fleming, I. Thiele, J.D. Orth, A.M. Feist, D.C. Zielinski, A. Bordbar, N.E. Lewis, S. Rahmanian, J. Kang, D.R. Hyduke, B.O. Palsson, Quantitative prediction of cellular metabolism with constraint-based models: the COBRA Toolbox v2.0, Nat. Protoc. 6 (2011) 1290–1307.
[43] C. Chen, H. Le, C.T. Goudar, An automated RNA-Seq analysis pipeline to identify and visualize differentially expressed genes and pathways in CHO cells, Biotechnol. Prog. 31 (2015) 1150–1162.
[44] F.C. Courtes, J. Lin, H.L. Lim, S.W. Ng, N.S. Wong, G. Koh, L. Vardy, M.G. Yap, B. Loo, D.Y. Lee, Translatome analysis of CHO cells to identify key growth genes, J. Biotechnol. 167 (2013) 215–224.
[45] W. Sommeregger, P. Mayrhofer, W. Steinfellner, D. Reinhart, M. Henry, M. Clynes, P. Meleady, R. Kunert, Proteomic differences in recombinant CHO cells producing two similar antibody fragments, Biotechnol. Bioeng. 113 (2016) 1902–1912.
[46] C. Xie, X. Mao, J. Huang, Y. Ding, J. Wu, S. Dong, L. Kong, G. Gao, C.Y. Li, L. Wei, KOBAS 2.0: a web server for annotation and identification of enriched pathways and diseases, Nucleic Acids Res. 39 (2011) W316–22.
[47] Y. Benjamini, Y. Hochberg, Controlling the false discovery rate a practical and powerful approach to multiple testing, J. R. Stat. Soc. 57 (1995) 289–300.
[48] D. Geoghegan, C. Arnall, D. Hatton, J. Noble-Longster, C. Sellick, T. Senussi, D.C. James, Control of amino acid transport into Chinese hamster ovary cells, Biotechnol. Bioeng. 115 (2018) 2908–2929.
[49] S. Pereira, H.F. Kildegaard, M.R. Andersen, Impact of CHO metabolism on cell growth and protein production: an overview of toxic and inhibiting metabolites and nutrients, Biotechnol. J. 13 (2018) e1700499.
[50] N. Carinhas, T.M. Duarte, L.C. Barreiro, M.J. Carrondo, P.M. Alves, A.P. Teixeira, Metabolic signatures of GS-CHO cell clones associated with butyrate treatment and culture phase transition, Biotechnol. Bioeng. 110 (2013) 3244–3257.
[51] F. Hartley, T. Walker, V. Chung, K. Morten, Mechanisms driving the lactate switch in Chinese hamster ovary cells, Biotechnol. Bioeng. 115 (2018) 1890–1903.
[52] T. Fu, C. Zhang, Y. Jing, C. Jiang, Z. Li, S. Wang, K. Ma, D. Zhang, S. Hou, J. Dai, G. Kou, H. Wang, Regulation of cell growth and apoptosis through lactate dehydrogenase C over-expression in Chinese hamster ovary cells, Appl. Microbiol. Biotechnol. 100 (2016) 5007–5016.
[53] T.M. Duarte, N. Carinhas, L.C. Barreiro, M.J. Carrondo, P.M. Alves, A.P. Teixeira, Metabolic responses of CHO cells to limitation of key amino acids, Biotechnol. Bioeng. 111 (2014) 2095–2106.
[54] C. Long, X. Zeng, J. Xie, Y. Liang, J. Tao, Q. Tao, M. Liu, J. Cui, Z. Huang, B. Zeng, High-level production of Monascus pigments in Monascus ruber CICC41233 through ATP-citrate lyase overexpression, Biochem. Eng. J. 146 (2019) 160–169.
[55] M.D. Neinast, C. Jang, S. Hui, D.S. Murashige, Q. Chu, R.J. Morscher, X. Li, L. Zhan, E. White, T.G. Anthony, J.D. Rabinowitz, Z. Arany, Quantitative analysis of the whole-body metabolic fate of branched-chain amino acids, Cell Metab. 29 (2019) 417–429 e4.
[56] A. Shrestha, E. Mullner, K. Poutanen, H. Mykkanen, A.A. Moazzami, Metabolic changes in serum metabolome in response to a meal, Eur. J. Nutr. 56 (2017) 671–681.
[57] Z.Z. Zhang, M.L. Fan, X. Hao, X.M. Qin, Z.Y. Li, Integrative drug efficacy assessment of Danggui and European Danggui using NMR-based metabolomics, J. Pharm. Biomed. Anal. 120 (2016) 1–9.
[58] J.S.A. Mattick, K. Kamisoglu, M.G. Ierapetritou, I.P. Androulakis, F. Berthiaume, Branched-chain amino acid supplementation: impact on signaling and relevance to critical illness, Wiley Interdiscip. Rev. Syst. Biol. Med. 5 (2013) 449–460.
[59] C.B. Newgard, Interplay between lipids and branched-chain amino acids in development of insulin resistance, Cell Metab. 15 (2012) 606–614.
[60] E.J. O'Brien, J.M. Monk, B.O. Palsson, Using genome-scale models to predict biological capabilities, Cell 161 (2015) 971–987.
[61] B.C. Mulukutla, J. Kale, T. Kalomeris, M. Jacobs, G.W. Hiller, Identification and control of novel growth inhibitors in fed-batch cultures of Chinese hamster ovary cells, Biotechnol. Bioeng. 114 (2017) 1779–1790.
[62] B.C. Mulukutla, J. Mitchell, P. Geoffroy, C. Harrington, M. Krishnan, T. Kalomeris, C. Morris, L. Zhang, P. Pegman, G.W. Hiller, Metabolic engineering of Chinese hamster ovary cells towards reduced biosynthesis and accumulation of novel growth inhibitors in fed-batch cultures, Metab. Eng. 54 (2019) 54–68.
[63] A. Salazar, M. Keusgen, J. von Hagen, Amino acids in the cultivation of mammalian cells, Amino Acids 48 (2016) 1161–1171.
[64] Z. Huang, S. Yoon, Integration of time-series transcriptomic data with genome-scale CHO metabolic models for mAb engineering, Processes 8 (2020) 331.